PHYSICAL REVIEW B VOLUME 43, NUMBER 16 1 JUNE 1991

Direct imaging of the oxygen sublattice in $YBa_2Cu_3O_{7-\delta}$ superconductors by high-resolution electron microscopy

Y. Yan* and M. G. Blanchin
Département de Physique des Matériaux, Université Claude Bernard, 69622 Villeurbanne CEDEX, France
(Received 25 February 1991)

Direct imaging of the oxygen sublattice in high-T_c $YBa_2Cu_3O_{7-\delta}$ superconductors by means of high-resolution transmission electron microscopy (HREM) has appeared difficult to achieve experimentally. Presented here are experimental HREM images along both the *a* and the *b* directions of the structure which have been obtained from thin crystals observed at 400 kV near the Scherzer defocus condition. In such micrographs the occupied oxygen columns are imaged as black dots clearly visible between the darker metal dots, whereas the oxygen vacancy columns are seen as bright dots. Thus, the [100] and [010] projections of the structure can be distinguished directly from the experimental HREM image. These direct structural images of the oxygen sublattice are consistent with the corresponding simulated images calculated on the basis of the $YBa_2Cu_3O_7$ orthorhombic structure proposed in the literature.

Many studies of the high-T_c superconductor materials $YBa_2Cu_3O_{7-\delta}$ have shown the critical influence of the oxygen concentration on the physical properties of these compounds.[1-3] Thus, the ability to detect the arrangement of the oxygen atoms in the structure is highly desirable. Neutron-diffraction experiments have allowed determination of the location of the long-range-ordered oxygen vacancies within the unit cell of $YBa_2Cu_3O_7$ (depicted in Fig. 1): One type of vacancies (hereafter referred to as V_1 type) is located at $(0,0,\frac{1}{2})$ in the Y planes, thus forming an arrangement with a two-dimensional character, and another type (hereafter referred to as V_2 type) is located at $(\frac{1}{2},0,0)$ in the Cu(1) planes, leading to the formation of one-dimensional chains.[4,5] Although neutron diffraction is a more-precise technique to determine atomic positions and occupancies, high-resolution transmission electron microscopy (HREM) allows imaging of the structure at high spatial resolution. A question that arose very early in HREM structural studies of $YBa_2Cu_3O_{7-\delta}$ superconductors was whether the oxygen sublattice could be imaged directly. There have been many efforts to characterize the oxygen ordering in these compounds by means of HREM.[6-10] From the features of the permutation twin,[6,11] we were able to differentiate the structural images along the *a* and the *b* axes of the structure in well-ordered $YBa_2Cu_3O_{7-\delta}$ microcrystals observed by HREM at 200 kV. However, the theoretical resolution reached at that voltage was not sufficient to visualize the oxygen sublattice. HREM images at 400 kV calculated by Krakow and Shaw showed that structure images of the oxygen sublattice can be obtained in thin crystals at the Scherzer defocus condition,[8] but the corresponding experimental images so predicted had not then been reported. Here, we present HREM images obtained at 400 kV along the *a* and the *b* directions of the $YBa_2Cu_3O_7$ structure which show the different distribu-

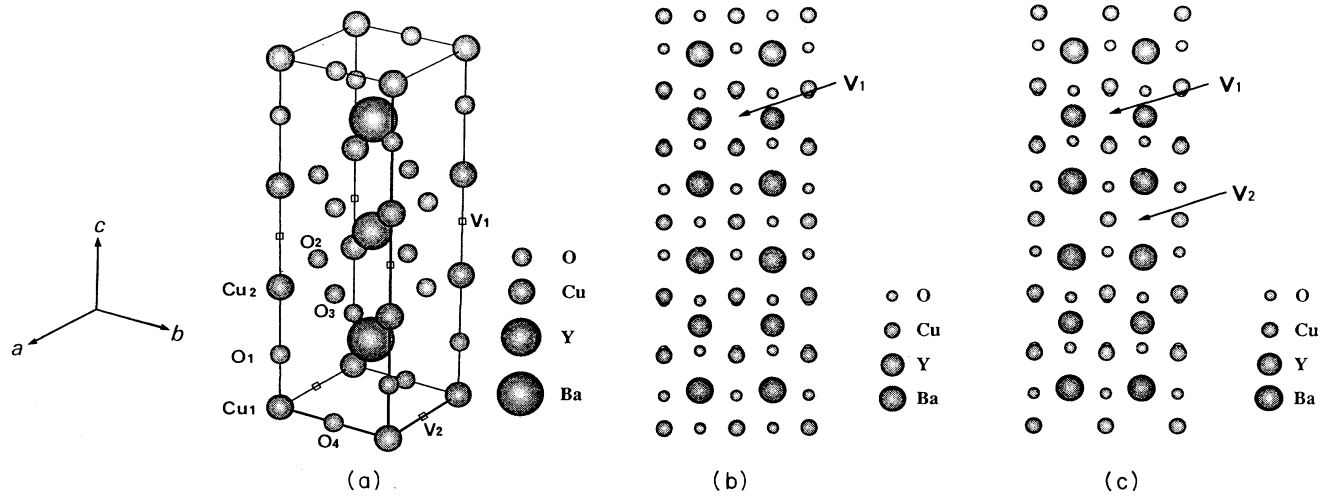

FIG. 1. (a) Model of the orthorhombic structure $YBa_2Cu_3O_7$: $a=0.38206$ nm, $b=0.38851$ nm, and $c=1.16757$ nm. (b) Structural projection along the [100] direction. (c) Structural projection along the [010] direction. Note that the tunnels from the V_1 oxygen vacancies in the Y planes are smaller than those from the V_2 vacancies in the Cu(1) planes.

tion of the oxygen atoms in the Cu(1) planes. The oxygen sublattice in high-T_c superconductors is directly imaged by HREM.

High-T_c superconductor $YBa_2Cu_3O_{7-\delta}$ ceramics were produced at Ecole Nationale Supérieure de Céramique Industrielle (ENSCI), Limoges, France, made from commercial powder by sintering. The specimens were prepared for microscopy by standard techniques for ceramic oxides and then immediately placed in the microscope to avoid water-vapor and oxygen contamination. HREM observations at room temperature were performed at Centre d'Études Nucléaires de Grenoble (CEN), Grenoble, France, using a JEOL-4000EX microscope at 400 kV with a top-entry double-tilting state ($\pm 15°$), capable of a theoretical resolution of 0.17 nm. Image simulations were carried out using a version of the SHRLI programs based on the multislice theory[12] (parameters: voltage, 400 kV; objective lens spherical aberration constant, 1.07 mm; beam divergence, 1 mrad; objective aperture, 1.1 $Å^{-1}$; 128×128 Fourier transform; Debye-Waller factors taken from the neutron-diffraction studied by Capponi *et al.*[5]).

A through-focus series of experimental micrographs (labeled EM) from the thin crystal edge and of simulated images (labeled SIM) along the *a* and the *b* axes (for a crystal thickness of 1.8 nm) are compared in Fig. 2. Reliable distinction cannot be made between the two series of micrographs, except at the optimum defocus, −48 nm (near the Scherzer value), where distinctive features can be viewed in the Cu(1) layer sandwiched by the darkest dots, corresponding to the heaviest Ba atoms. In the micrograph taken along the *b* axis [Fig. 2(b)], bright dots are seen between the Ba and the Cu(1) columns, which correspond to the V_2-type oxygen vacancy tunnels, whereas dark dots corresponding to the O(4)-occupied oxygen columns appear in the micrograph taken along the *a* axis [Fig. 2(a)]. The contrast features of the experimental images are well fitted by those of the simulated images along the *a* and the *b* axes [Figs. 2(c) and 2(d), respectively], which are consistent with the data drawn from x-ray and neutron-diffraction studies (Fig. 1). The variation in the image contrast of the through-focus series in Fig. 2 can be readily interpreted from the contrast transfer function of the microscope depending on defocus, as discussed previously.[13]

Further enlargement (Fig. 3) of the experimental images of Fig. 2 obtained at the optimum defocus reveals that the oxygen columns in both projections are imaged as weaker dots between the very dark dots corresponding to the Y, Ba, and Cu columns. In the plane sandwiched by the Ba atoms, both the Cu(1) and O(4) columns are imaged as black dots in the projection along the *a* axis [Fig. 3(a)], whereas only the dark dots corresponding to the Cu(1) columns are seen in the micrograph obtained along the *b* axis [Fig. 3(b)]. Although the tunnels corresponding to the V_1 vacancy columns in the Y planes are smaller than those corresponding to the V_2 vacancy columns [see Fig. 1(b) and 1(c)], they appear as bright spots regularly distributed in the Y planes in Figs. 3(a) and 3(b); the corresponding distribution of oxygen vacancies in the material is thus directly confirmed by HREM. Further inspection shows that the distance between Ba and Ba atoms along the *c* axis is longer than that between Ba and Y (or Y and Ba) atoms, and the distance between Cu(1)-Cu(1) atoms on both sides of the Y planes is shorter than that between Cu(1)-Cu(2) atoms across the Ba planes, in agreement with the results from neutron- and x-ray-diffraction studies.

However, it can be observed in Fig. 3 that locally the intensity of some dots in the experimental images does not

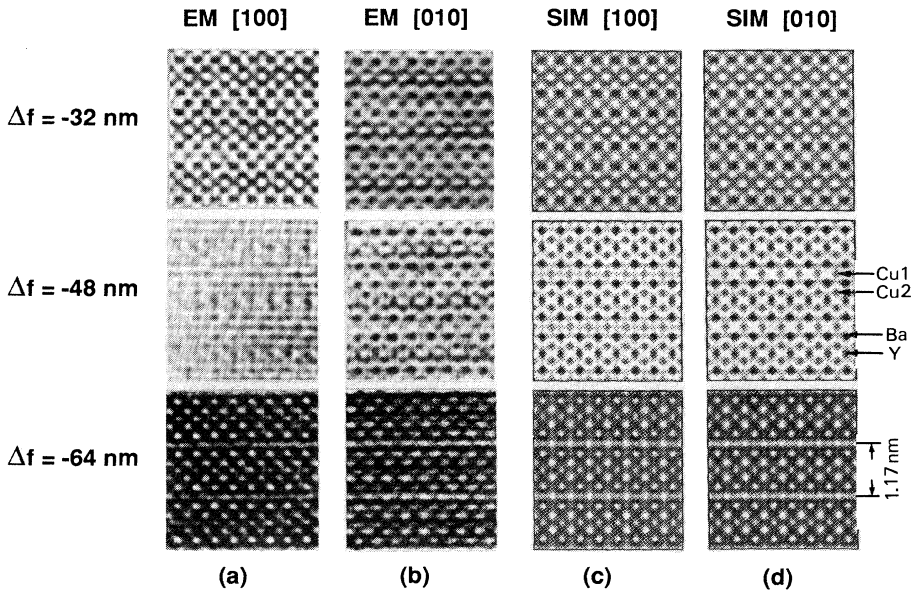

FIG. 2. Through-focus series of experimental micrographs (EM) and computer simulated images (SIM) from the specimen observed at 400 kV for a crystal thickness 1.8 nm: (a) experimental images along the [100] direction, (b) experimental images along the [010] direction, (c) simulated images along the [100] direction, and (d) simulated images along the [010] direction.

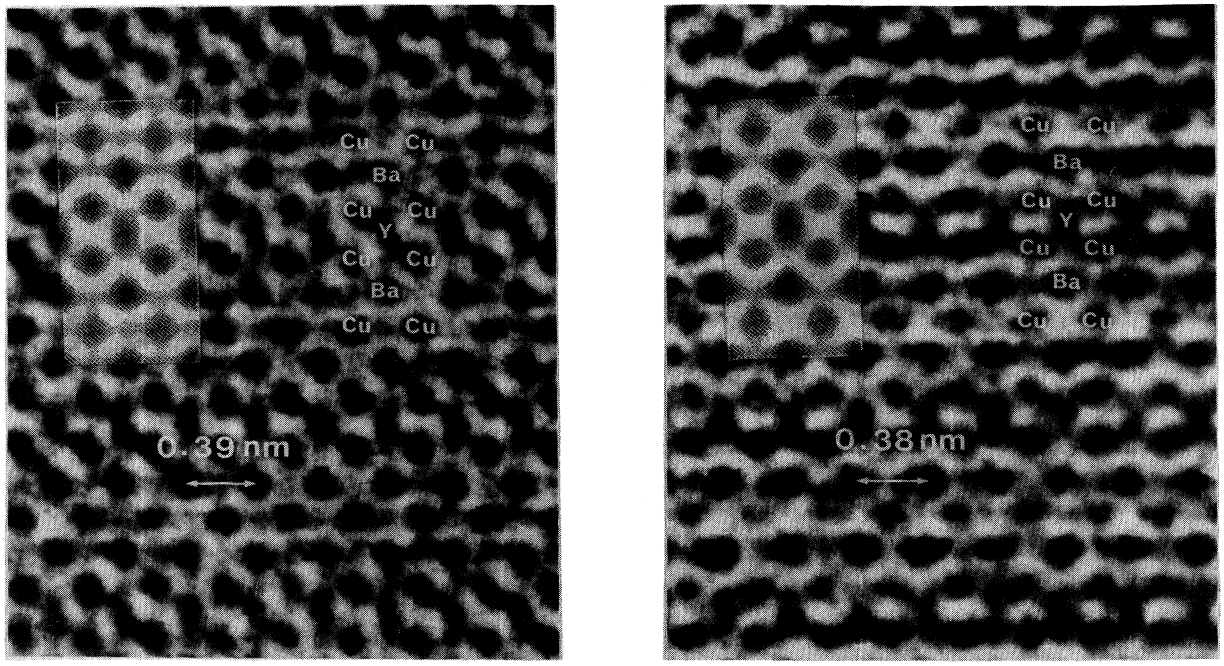

(a) (b)

FIG. 3. (a) Enlargement of a structure image along the [100] axis. Inset: simulated image (crystal thickness $t=1$ nm, $\Delta f=-48$ nm). (b) Enlargement of a structure image along the [010] axis. Inset: simulated image (crystal thickness $t=1.4$ nm, $\Delta f=-48$ nm).

match exactly the results of the image simulations. There are several possible explanations. Sample preparation by grinding may introduce local thickness variation in these ceramic materials. This will have a large influence on the intensity of the HREM image from such thin crystals: For instance, the scattering factor of Cu is only 25% smaller than that of Y. On the other hand, the contrast in the HREM images, especially that arising from the oxygen sublattice, appeared to be seriously influenced by the effects of electron-beam irradiation at 400 kV (induced atomic mobility, possible contamination, etc.). Our observations showed that the structure images were stable under the beam only within a very short time (less than 2–3 min), which was consistent with the results reported by Bursill, Peng, and Sellar.[14] Accordingly, the micrographs reproduced here have been obtained after extremely short irradiation times. A series of experimental micrographs exhibiting the irradiation effects have also been obtained, and systematic study of the influence of these effects and of the imaging parameters on the HREM image contrast will be reported later in more details.

We thank Dr. D. S. Smith (ENSCI) for providing the samples and Dr. A. Bourret for permitting us to use the 400-kV microscope at CEN, Grenoble, France. Dr. J. M. Penisson (CEN, Grenoble) is gratefully thanked for kind and stimulating discussions. The Département de Physique des Matériaux is "Unité Associée au Centre National de la Recherche Scientifique No. 172."

*On leave from Laboratory of Solid State Microstructures, Nanjing University, Peoples Republic of China.

[1]A. L. Robinson, Sci. Res. News **256**, 1063 (1987).
[2]R. Beyer, G. Lim, E. M. Engler, R. J. Savoy, T. M. Shaw, T. R. Dinger, W. J. Gallagher, and R. L. Sandstrom, Appl. Phys. Lett. **50**, 1918 (1987).
[3]R. J. Cava, B. Batlogg, C. H. Chen, E. A. Rietman, S. M. Zaharak, and D. Werder, Nature (London) **329**, 423 (1987).
[4]M. A. Beno, L. Soderholm, D. W. Capone II, D. G. Hinks, J. D. Jorgensen, I. K. Schuller, C. U. Segre, K. Zhang, and J. D. Grace, Appl. Phys. Lett. **51**, 57 (1987).
[5]J. J. Capponi, C. Chaillout, A. W. Hewat, P. Lejay, M. Marezio, N. Nguyen, B. Raveau, J. L. Soubeyroux, J. L. Tholence, and R. Tournier, Europhys. Lett. **3**, 1301 (1987).
[6]Y. Yan and M. G. Blanchin, Philos. Mag. A **61**, 513 (1990).
[7]A. Ourmazd and J. C. H. Spence, Nature (London) **329**, 425 (1987).
[8]W. Krakow and T. M. J. Shaw, J. Electron Microsc. Tech. **8**, 273 (1988).
[9]N. P. Huxford, D. J. Eaglesham, and C. J. Humphreys, Nature (London) **329**, 812 (1987).
[10]H. Shibahara, J. P. Zhang, and L. D. Marks, Ultramicroscopy **27**, 185 (1989).
[11]Y. Yan, M. G. Blanchin, and A. Wicker, Physica C **175**, 651 (1991).
[12]M. A. O'Keefe, P. R. Busek, and S. Iijima, Nature (London) **274**, 322 (1978).
[13]Y. Yan and M. G. Blanchin, Philos. Mag. Lett. **62**, 311 (1990).
[14]L. A. Bursill, Peng JuLin, and J. R. Sellar, Mater. Forum **14**, 41 (1990).

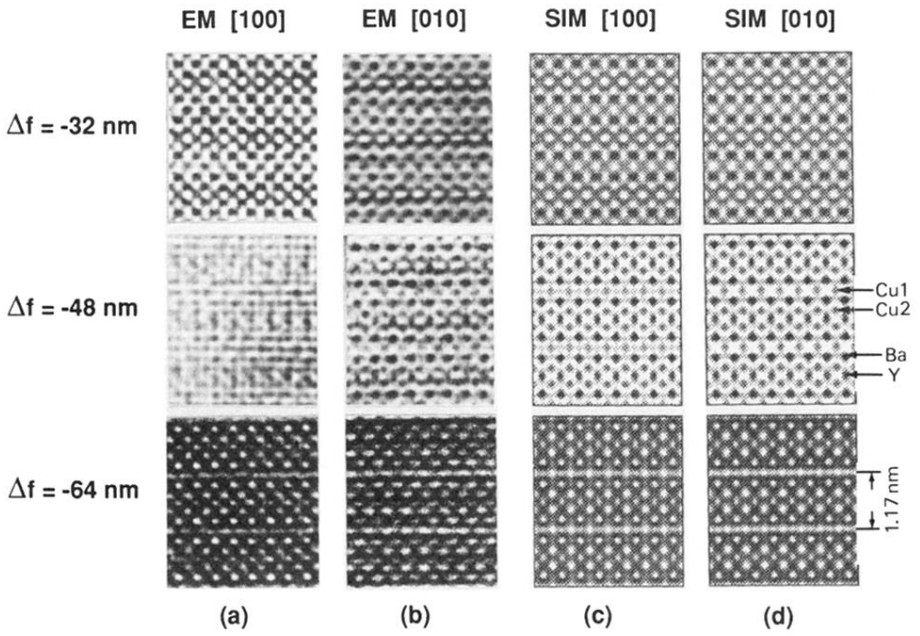

FIG. 2. Through-focus series of experimental micrographs (EM) and computer simulated images (SIM) from the specimen observed at 400 kV for a crystal thickness 1.8 nm: (a) experimental images along the [100] direction, (b) experimental images along the [010] direction, (c) simulated images along the [100] direction, and (d) simulated images along the [010] direction.

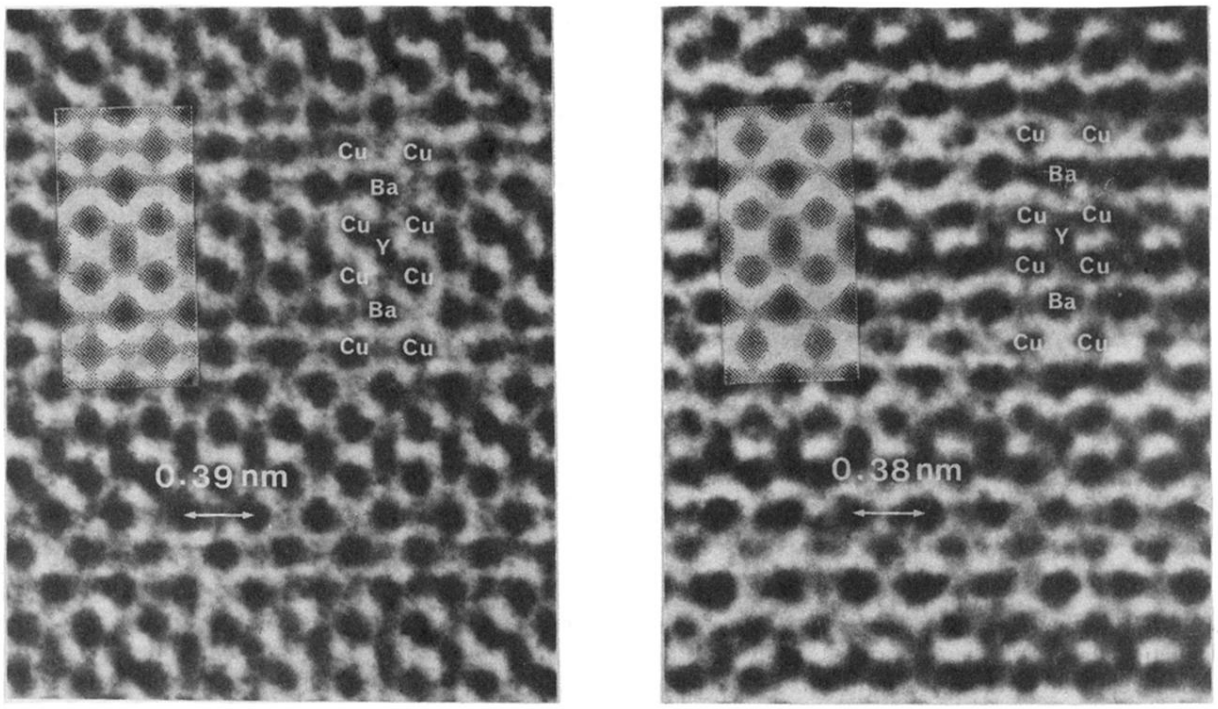

(a) (b)

FIG. 3. (a) Enlargement of a structure image along the [100] axis. Inset: simulated image (crystal thickness $t = 1$ nm, $\Delta f = -48$ nm). (b) Enlargement of a structure image along the [010] axis. Inset: simulated image (crystal thickness $t = 1.4$ nm, $\Delta f = -48$ nm).